Superconducting Circuits and Quantum Computation

Academic and Research Staff
Professor Terry P. Orlando

Collaborators
Prof. Leonid Levitov, Prof. Seth Lloyd, Prof. Johann E. Mooij[1], Dr. Juan J. Mazo[2], Dr. Fernando F. Falo[2], Dr. Karl Berggren[3], Prof. M. Tinkham[4], Nina Markovic[4], Sergio [4], Prof. Marc Feldman[5], Prof. Mark Bocko[5], Jonathon Habif[5]

Visiting Scientists and Research Affiliates
Dr. Juan Mazo[2], Prof. Johann E. Mooij[1], Dr. Kenneth J. Segall, Dr. Enrique Trías

Graduate Students
Donald S. Crankshaw, Daniel Nakada, Lin Tian, Janice Lee, Bhuwan Singh, David Berns

Undergraduate Students
Andrew S. Kuziemko, Michael O'Hara

Support Staff
Scott Burris

Introduction

Superconducting circuits are being used as components for quantum computing and as model systems for non-linear dynamics. Quantum computers are devices that store information on quantum variables and process that information by making those variables interact in a way that preserves quantum coherence. Typically, these variables consist of two quantum states, and the quantum device is called a quantum bit or qubit. Superconducting quantum circuits have been proposed as qubits, in which circulating currents of opposite polarity characterize the two quantum states. The goal of the present research is to use superconducting quantum circuits to perform the measurement process, to model the sources of decoherence, and to develop scalable algorithms. A particularly promising feature of using superconducting technology is the potential of developing high-speed, on-chip control circuitry with classical, high-speed superconducting electronics. The picosecond time scales of this electronics means that the superconducting qubits can be controlled rapidly on the time scale and the qubits remain phase-coherent.

Superconducting circuits are also model systems for collections of coupled classical non-linear oscillators. Recently we have demonstrated a ratchet potential using arrays of Josephson junctions as well as the existence of a novel non-linear mode, known as a discrete breather. In addition to their classical behavior, as the circuits are made smaller and with less damping, these non-linear circuits will go from the classical to the quantum regime. In this way, we can study the classical-to-quantum transition of non-linear systems.

[1] Delft University of Technology, The Netherlands
[2] University of Saragoza, Spain
[3] M.I.T. Lincoln Lab
[4] Harvard University
[5] University of Rochester

1. Superconducting Persistent Current Qubits In Aluminum

Sponsors
AFOSR grant F49620-1-1-0457 funded under the Department of Defense, Defense University Research Initiative on Nanotechnology (DURINT) and by ARDA; DOD and AFOSR; ARO GrantDAAG55-98-1-0369

Project Staff
Lin Tian, Donald Crankshaw, Daniel Nakada, and Caspar H. van der Wal[1], Professor Leonid Levitov, Professor Seth Lloyd, Professor Johan E. Mooij[1], Professor Kees Harmans[1], Alexander C.J. ter Haar[1], Frank Wilhelm[1], Raymond N. Schouten[1], and Professor Terry P. Orlando[2]

Quantum computers are devices that store information on quantum variables such as spin, photons, and atoms, and process that information by making those variables interact in a way that preserves quantum coherence. Typically, these variables consist of two-state quantum systems called quantum bits or 'qubits'. To perform a quantum computation, one must be able to prepare qubits in a desired initial state, coherently manipulate superpositions of a qubit's two states, couple qubits together, measure their state, and keep them relatively free from interactions that induce noise and decoherence.

We have designed a superconducting qubit that has circulating currents of opposite sign as its two states. The circuit consists of three nano-scale aluminum Josephson junctions connected in a superconducting loop and controlled by magnetic fields.

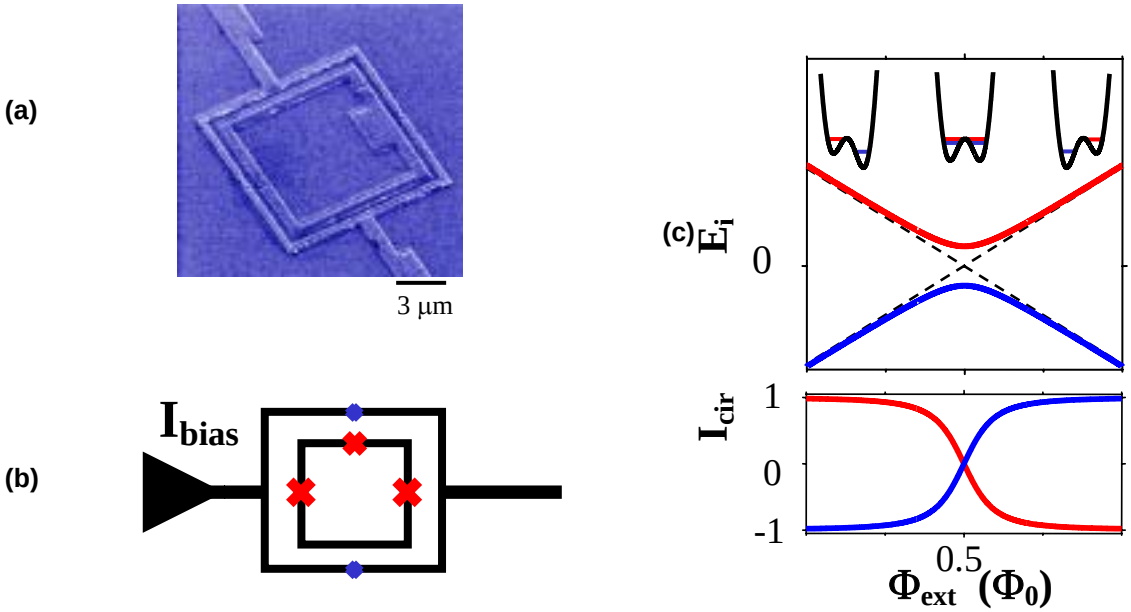

FIGURE 1. (a) SEM image of the persistent current qubit (inner loop) surrounded by the measuring dc SQUID. (b) a schematic of the qubit and measuring SQUID, the x's mark the Josephson junctions. (c) The energy levels for the ground state (dark line) and the first excited state of the qubit versus applied flux. The double well potentials are shown schematically above. The lower graph shows the circulating current in the qubit for both states as a function of applied flux. The units of flux are given in terms of the flux quantum.

[1] Delft University of Technology, The Netherlands

Figure 1a shows a SEM image of the persistent current qubit (inner loop) and the measuring dc SQUID (outer) loop. The Josephson junctions appear as small "breaks" in the image. A schematic of the qubit and the measuring circuit is shown in Figure 1b, where the Josephson junctions are denoted by x's. The qubit loop is 5×5 μm^2 with aluminum-oxide tunnel junctions, microfabricated at the TU Delft, by a shadow evaporation technique. (This is in contrast to the samples fabricated at MIT's Lincoln Laboratory that are made in niobium by photolithographic techniques on a trilayer of niobium-aluminum oxide-niobium wafer.) The capacitance of the junction is estimated to be about 3 fF and the ratio of the Josephson energy to the charging energy is about 40. The inductances of the inner qubit loop and the outer measuring loop are about 11 and 16 pH respectively, with a 7 pH mutual inductive coupling.

The energy levels of the ground state (dark line) and the first excited state (light line) are shown in Figure 1c near the applied magnetic field of 0.5 Φ_0 in the qubit loop. Classically the Josephson energy of the two states would be degenerate at this bias magnetic field and increase and decrease linearly from this bias field, as shown by the dotted line. Since the slope of the *E* versus magnetic field is the circulating current, we see that these two classical states have opposite circulating currents. However, quantum mechanically, the charging energy couples these two states and results in a energy level repulsion at Φ_{ext} = 0.5 Φ_0, so that there the system is in a linear superposition of the currents flowing in opposite directions. As the applied field is changed from below Φ_{ext} = 0.5 Φ_0 to above, we see that the circulating current goes from negative, to zero at Φ_{ext} = 0.5 Φ_0, to positive as shown in the lower graph of Figure 1c. This flux can be measured by the sensitive flux meter provided by the dc SQUID.

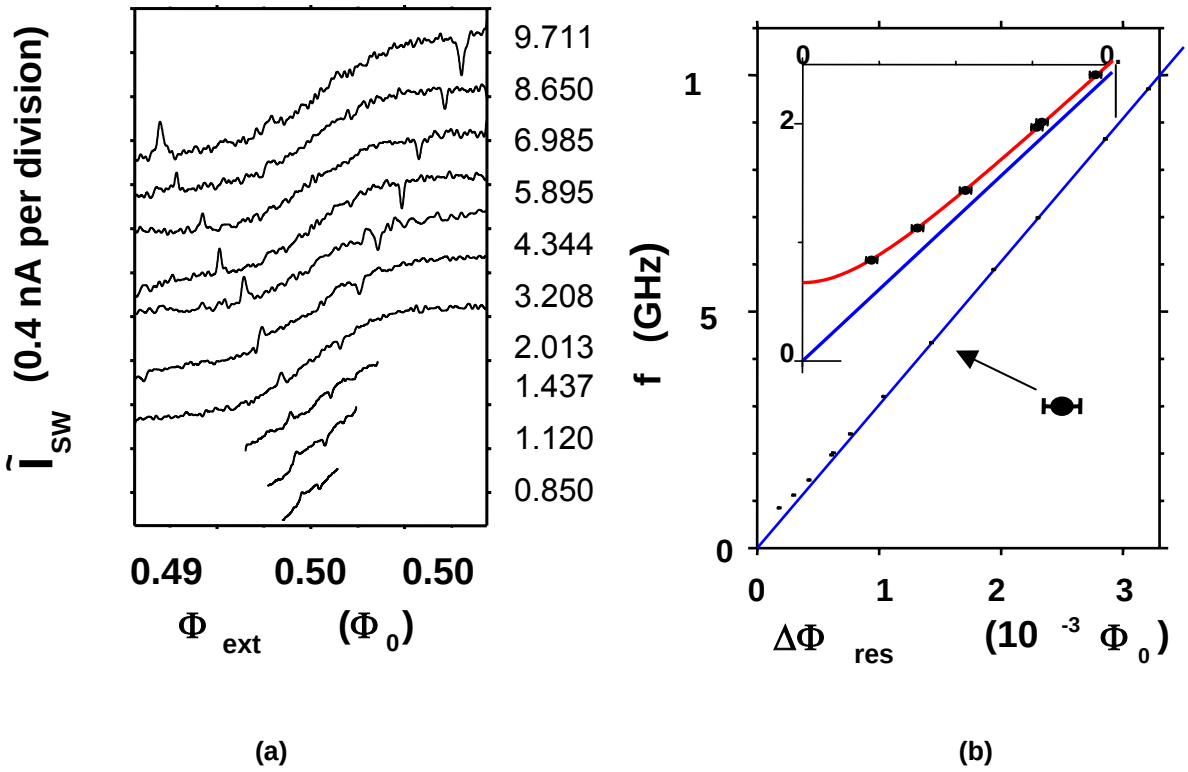

FIGURE 2. (a) The circulating current as inferred from the dc SQUID measurements for various applied microwave frequencies. The curves are offset for clarity. (b) Half the distance in Φ_{ext} measured between the resonant peaks and the dips at different frequencies *f*. The inset shows the low frequency data points. The grey line is a linear fit through the high frequency points and zero. The black line is a fit of the quantum theory.

Figure 2a shows the circulating current as inferred from the dc SQUID measurements for various applied microwave frequencies. The curves are offset for clarity, and each curve shows the expected change from negative circulating current at low applied flux, to zero at half a flux quantum, and then to positive current at higher flux. This clearly shows that the qubit has the change in flux profile expected of the ground state. When microwaves are applied at the energy difference matching the difference between the ground state and the first excited state, then a transition is induced from the ground state to the first excited state. These are shown by the resonant-like structures in each curve. A plot of the distance in Φ_{ext} at the resonance from Φ_{ext} = 0.5 Φ_0 is shown in the figure on the left. Quantum mechanically the energy is expected to follow the form

$$\Delta E = \sqrt{\left[2I_p\left(\Phi_{ext} - 0.5\Phi_0\right)\right]^2 + \left(2V\right)^2}$$

where I_p is the circulating current and V is the tunneling matrix element between the two circulating current states at Φ_{ext} = 0.5 Φ_0. The inset shows a fit to the curve which gives an energy gap of about 600 MHz and a circulating current of about 500 nA as expected. These results are among the first experimental verification of the superposition of macroscopic circulating current states.

2. Superconducting Persistent Current Qubits in Niobium

Sponsors
AFOSR grant F49620-1-1-0457 funded under the Department of Defense, Defense University Research Initiative on Nanotechnology (DURINT) and by ARDA; DOD and AFOSR; ARO GrantDAAG55-98-1-0369

Project Staff
Ken Segall, Daniel Nakada, Donald Crankshaw, Bhuwan Singh, Janice Lee, Karl Berggren (Lincoln Laboratory), Nina Markovic and Sergio Valenzuela (Harvard); Professors Terry Orlando, Leonid Levitov, Seth Lloyd and Professor Michael Tinkham (Harvard)

Quantum Computation is an exciting idea whose study combines the exploration of new physical principles with the development of a new technology. In these early stages of research one would like to be able to accomplish the manipulation, control and measurement of a single two-state quantum system while maintaining quantum coherence. This will require a coherent two-state system (a qubit) along with a method of control and measurement. Superconducting quantum computing has the promise of an approach that could accomplish this in a manner that can be scaled to large numbers of qubits. We are studying the properties of a two-state system made from a niobium (Nb) superconducting loop, which can be incorporated on-chip with other superconducting circuits to perform the control and measurement. The devices we study are fabricated at Lincoln Laboratory, which uses a Nb-trilayer process for the superconducting elements and photolithography to define the circuit features. Our system is thus inherently scalable but has the challenge of being able to demonstrate appreciable quantum coherence.

The particular device that we have studied so far is made from a loop of Nb interrupted by 3 Josephson junctions. The application of an external magnetic field to the loop induces a circulating current whose magnetic field either adds to (say circulating current in the clockwise direction) or opposes (counterclockwise) the applied magnetic field. When the applied field is near to one-half of a flux quantum, both the clockwise and counterclockwise current states are classically stable. The system behaves as a two-state system. The potential energy versus circulating current is a so-called double-well potential (see Fig.2), with the two minima representing the two states of equal and opposite circulating current. A SQUID magnetometer inductively coupled to the qubit can be used to measure the magnetic field caused by the circulating current and thus determine the state of the qubit. The SQUID has a switching current which depends very sensitively on magnetic field. When the magnetic field from the qubit adds to the external field we observe a smaller switching current; when it subtracts from the external

field we observe a smaller larger current. We measure the switching current by ramping up the bias current of the SQUID and recording the current at which it switches. Typically a few hundred such measurements are taken. We have performed these measurements versus magnetic field, temperature and SQUID ramping rate.

In the upper plot of Fig. 1 we show the average switching current versus magnetic field for our qubit-SQUID system. The SQUID switching current depends linearly on the applied magnetic field. A step-like transition occurs when the circulating current in the qubit changes sign, hence changing whether its magnetic field adds to or subtracts from the applied field. In Fig. 1 the qubit field adds to the SQUID switching current at lower fields (< 3mG) but subtracts from it at higher fields (>3mG). Each point in the upper curve is an average of 1000 single switching current measurements. If we look at a histogram of the 1000 switching currents in the neighborhood of the transition, we discover that it represents a joint probability distribution. Two distinct switching currents representing the two states of the qubit can be clearly resolved. Changing the magnetic field alters the probability of being measured in one state or the other.

In Fig. 2 we show the potential energy for the system as we sweep through the transition. (We used a different assignment for “zero” field in Fig. 2 than Fig. 1, which is why the step occurs at a different magnetic field value). In the first part of the transition the system has a higher probability of being measured in the left well, which corresponds to the circulating current state which adds to switching current of the SQUID. At the midpoint of the transition the system is measured in both wells with equal probability. At higher fields the system has a larger probability of being measured in the right well. The mechanism for the system to move between the wells at these temperatures (>300 mK) is thermal activation. We have measured the system at lower temperatures, and there the mechanism is unclear. The focus of our future efforts is to determine if the mechanism changes to quantum mechanical tunneling at lower temperatures and how coherent the tunneling can be. If we are successful that will be the first indication that superconducting quantum computers in Nb are possible.

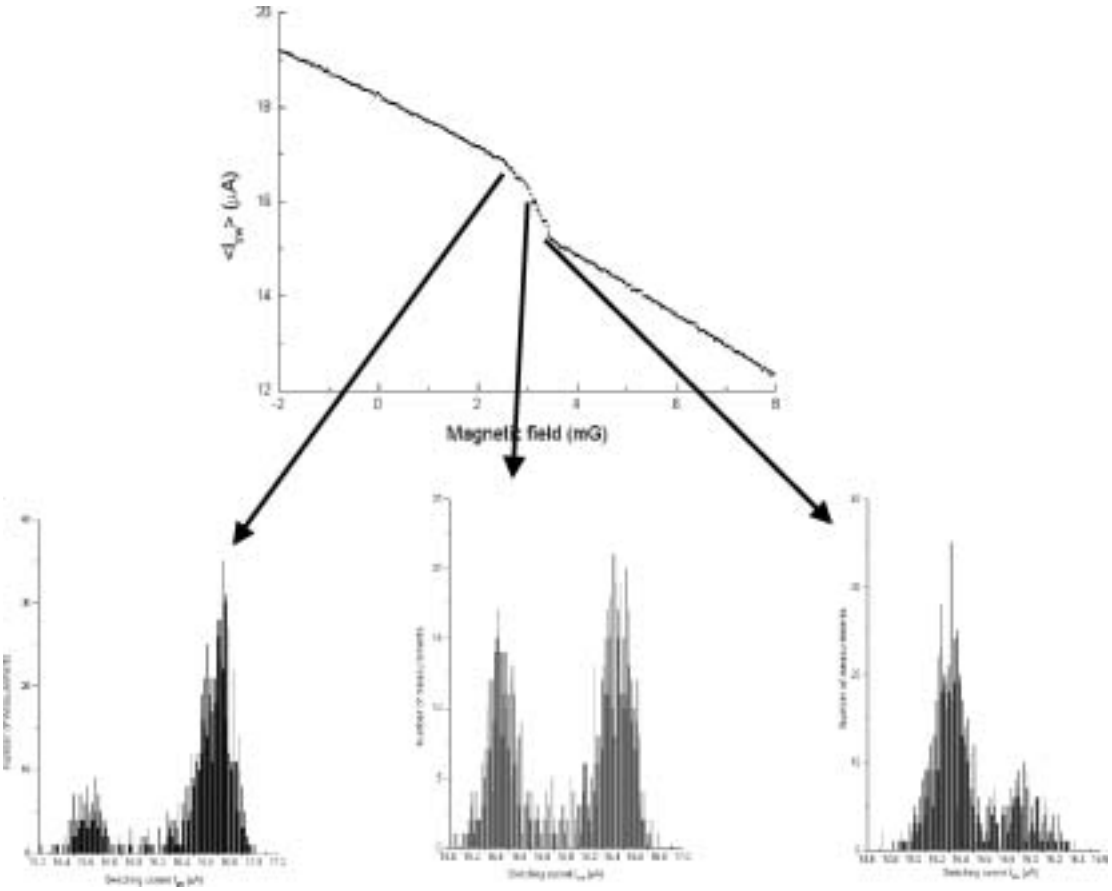

Fig. 1: Measurements of the switching current of the SQUID versus magnetic field.

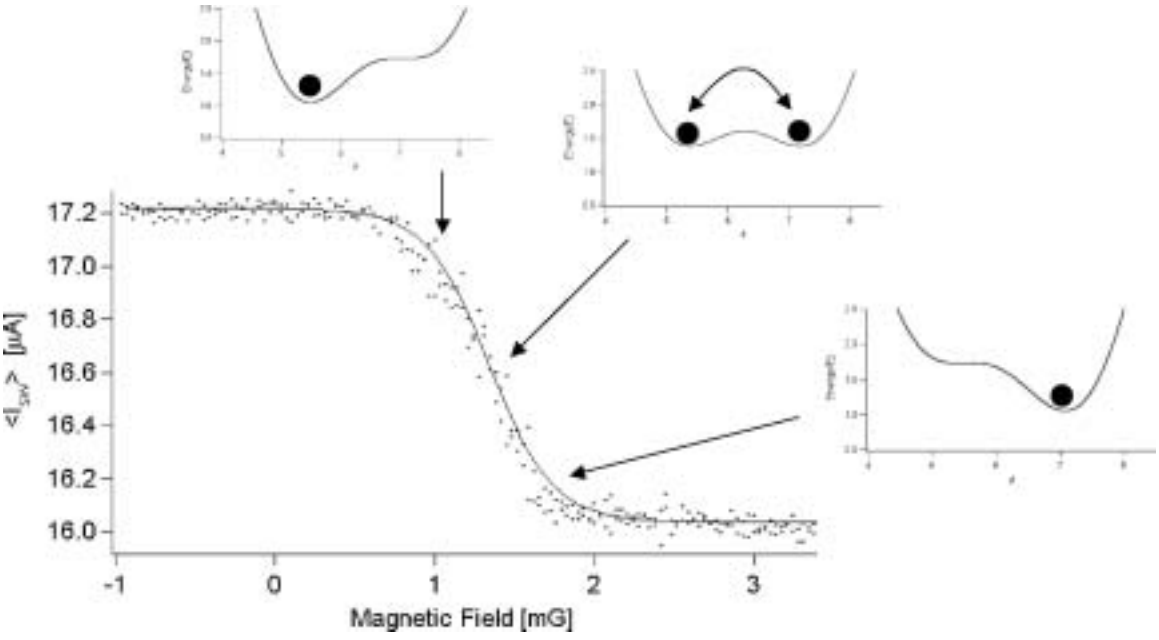

Fig. 2: Switching current versus magnetic field with the background field of the SQUID subtracted off.

3. Improved Critical-Current-Density Uniformity of Nb Superconducting Fabrication Process Using Anodization

Personnel
Daniel Nakada, T.P. Orlando, Karl K. Berggren (Lincoln Laboratory), Earle Macedo (Lincoln Laboratory)

Sponsors
AFOSR grant F49620-1-1-0457 funded under the Department of Defense, Defense University Research Initiative on Nanotechnology (DURINT) and by ARDA; DOD and AFOSR; ARO GrantDAAG55-98-1-0369

We studied an anodization technique for a Nb/Al/AlO_x/Nb trilayer process which provides a significant improvement in critical-current-density J_c uniformity across a 150-mm-diameter wafer. Anodization is an electrolytic process in which the surface of a metal is converted to its oxide form, this metal oxide layer serves as a protective barrier to further ionic or electron flow. The superconducting Josephson junctions were fabricated in a class-10 cleanroom facility at MIT Lincoln Laboratory. The Nb superconducting process uses optical projection lithography, chemical mechanical planarization of two oxide layers, a self-aligned via process and dry reactive ion etching (RIE) of the Nb and oxide layers. The most critical step in the fabrication process however is the definition of the tunnel junction. The junction consists of two Nb layers, the base electrode (B.E.) and counter-electrode (C.E.) separated by a thin AlO_x barrier. Fig. 1a shows a cross-section of the Josephson junction region after RIE is performed on the counter-electrode. After RIE, the junction edges are exposed to the atmosphere and are therefore vulnerable to chemical and/or plasma damage. Anodization is useful in minimizing damage to the junction region (Fig. 1b).

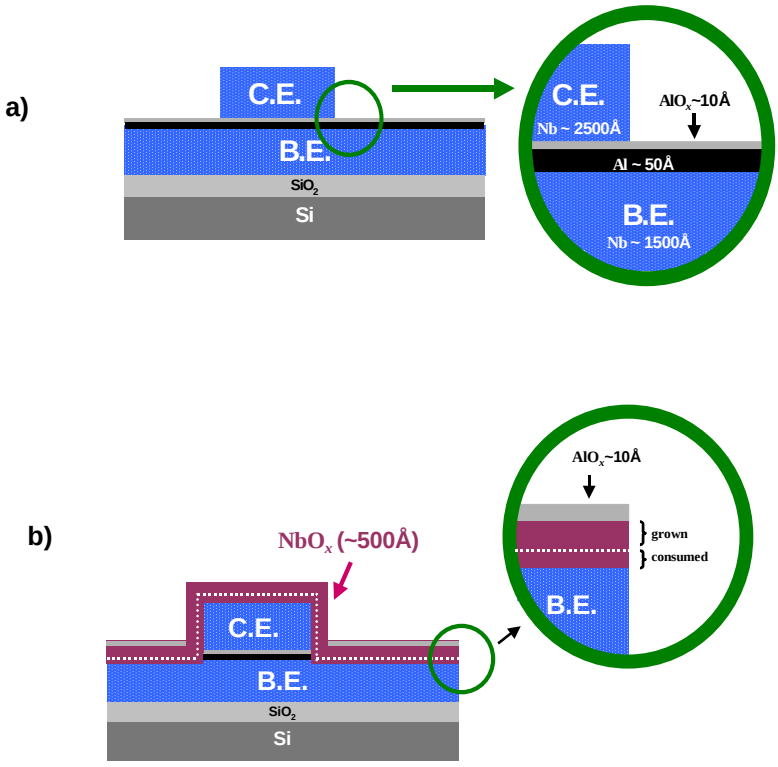

Fig 1. a) Nb Josephson junction region after counter-electrode is etched, b) After anodization, the junction edges are protected by a thick NbO_x layer.

Critical current I_c measurements of Josephson junctions were performed at room temperature using specially designed test structures. We used an automatic probing station to determine the I_c values of junctions across the entire wafer. The J_c uniformity of anodized/unanodized wafer pairs, fabricated together, were compared. The cross-wafer standard deviation of J_c was typically ~ 5% for anodized wafers but was /15% for unanodized wafers(Fig. 2). A low variation in J_c results in a higher yield of device chips per wafer with the desired current density. As a result of the improved cross-wafer distribution, the cross-chip uniformity is greatly improved as well; typically $<$ 1% for anodized chips. Low cross-chip J_c variation is needed for fast digital superconducting electronics.

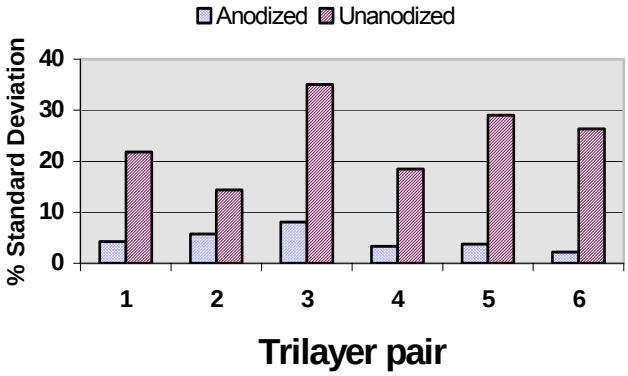

Fig 2. Comparison of standard deviation of the critical current density J_c across a wafer for pairs of wafers that were fabricated together except for the anodization step.

4. Decoherence of an On-chip Oscillator

Sponsors
AFOSR grant F49620-1-1-0457 funded under the Department of Defense, Defense University Research Initiative on Nanotechnology (DURINT) and by ARDA; DOD and AFOSR; ARO GrantDAAG55-98-1-0369

Project Staff
Lin Tian, Donald Crankshaw, Professor Seth Lloyd, Professor Terry P. Orlando

The two devices which have the most intimate connection to the qubit are the proposed on-chip oscillator and the DC SQUID. Designing these devices requires not just concern for proper operation, but for minimum decoherence as well.

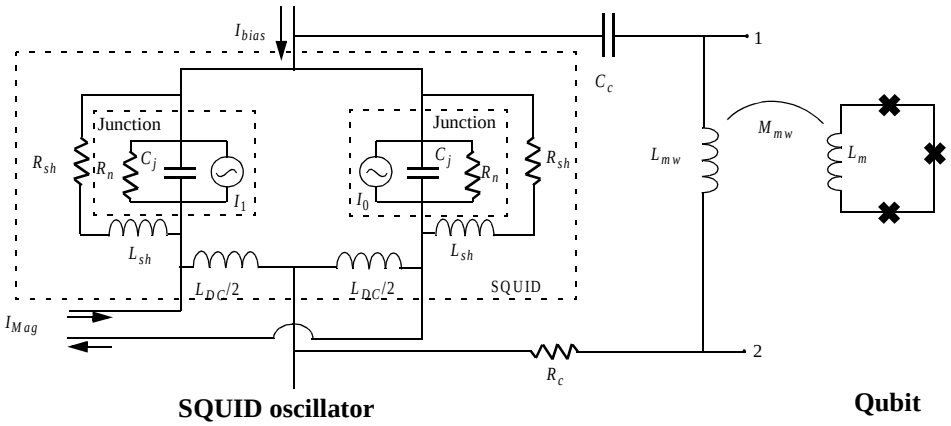

FIGURE 1. Circuit diagram of the SQUID oscillator coupled to the qubit. The SQUID contains two identical junctions, here represented as independent current sources and the RCSJ model, shunted by a resistor and inductor (R_{sh} and L_{sh}). A large superconducting loop (L_{mw}) provides the coupling to the qubit. The capacitor, C_c, prevents the DC current from flowing through this line, and the resistance, R_c, damps the resonance. Z_t, the impedance seen by the qubit, is the impedance across the inductor, Z_{12}.

The oscillator in Figure 1 is a simple overdamped DC SQUID. This gives two parameters with which to control the frequency and amplitude of the source: the bias current and the magnetic flux through the SQUID. In this design, the SQUID is placed on a ground plane to minimize any field bias from an external source, and direct injection supplies the flux by producing excess current along a portion of the SQUID loop. When a Josephson junction is voltage biased, its current oscillates at a frequency of $V_{bias}/\Phi$with an amplitude of I_c. For a stable voltage bias, this looks like an independent AC current source. In this circuit, the junction is current biased, and its oscillating output produces fluctuations in the voltage across the junction. Thus the DC voltage, approximately equal to *IbiasRsh*, gives the fundamental frequency, while harmonics distort the signal. If the shunt is small, such that $V_{bias}>>I_c|R_{sh}+j\omega L_{sh}|$, the voltage oscillations are small relative to the DC voltage and the higher harmonics become less of a problem. This allows us to model the junctions as independent sources (I_0 and I_1) in parallel with the RCSJ model. A DC SQUID with a small self inductance behaves much like a single junction whose I_c can be controlled by the flux through its loop. The circuit model is shown in Figure 1. This is similar in concept to our previous work with array oscillators. The impedance seen by the qubit is given by:

$$Z_t(\omega) = \left[\left(\frac{1/2}{j\omega C_j + \frac{1}{R_n} + \frac{1}{R_{sh} + j\omega L_{sh}}} + \frac{1}{j\omega C_c} + R_c \right)^{-1} + \frac{1}{j\omega L_{mw}} \right]^{-1}$$

This value comes from placing the other elements of the circuit in parallel with the inductance. The maximum amplitude of the oscillating magnetic flux is at the resonance of the RLC circuit consisting of R_c, C_c, and L_{mw}. In this case, the LC resonance occurs at 8.6 GHz. Directly on resonance, the SQUID produces high amplitude oscillations with a short dephasing time. Moving it off resonance lowers the amplitude but lengthens the dephasing time, as shown in Figure 2.

Table 1. SQUID oscillator parameters

I_c	R_n	C_j	R_{sh}	L_{sh}	R_c	C_c	L_{mw}	M_{mw}
260 μA	7.3 Ω	2100 fF	0.19 Ω	0.38 pH	0.73 Ω	4600 fF	75 pH	0.6 pH

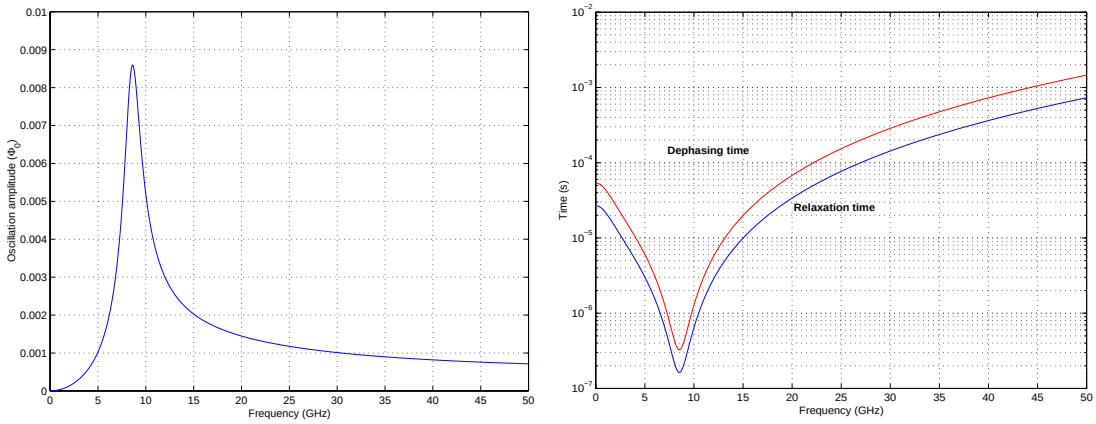

(a) **(b)**

FIGURE 2. Graphs showing the amplitude produced by the oscillator (a) and the decoherence times caused by the oscillator (b) as a function of frequency.

The noise from the DC SQUID shown in Figure 3 has a more complex relationship with the qubit decoherence. Since the resistive noise source is located outside of the SQUID, the noise contribution is evenly divided between the two branches. As the bias current is increased, however, the combination of circulating current and bias current creates different linear characteristics in the branches. The internal phase variable, $\varphi_{int}=(\varphi_1-\varphi_2)/2$, is driven by the external flux, so that $\varphi_{int} = \pi\bar{\Phi}\Phi 0$. This is considered a constant. φ_{ext} follows the bias current. While *I cir* directly couples to the qubit, environmental noise appears as fluctuations in the *I bias*. The fluctuations in *I bias* can be translated into fluctuations of *I cir* through Equation (2).

$$\delta I_{bias} = 2I_{c0}\cos\varphi_{\text{int}}\cos\overline{\varphi}_{ext}\delta\varphi_{ext}$$
$$\delta I_{cir} = I_{c0}\sin\varphi_{\text{int}}\sin\overline{\varphi}_{ext}\delta\varphi_{ext}$$

By translating the noise seen on the external phase variable into noise in the circulating current, which couples to the qubit, we can derive the spectral density in Equation (3), from which we derive decoherence and dephasing times.

$$J(\omega) = \left(\frac{2e}{\hbar}\right)^2 \frac{4}{\hbar\omega}\left(MI_p I_{bias}\tan\varphi_{\text{int}}\right)^2 \Re\{Z_t(\omega)\}$$

$Z_t(\omega)$ the impedance of the external environment. This is very similar to the above use of $Z_t(\omega)$, where it was the external environment seen across the inductor, except that in this case, the external environment includes the SQUID itself (its Josephson inductance and capacitance must be included, along with any external capacitance and resistance from the environment). Notice that the decoherence caused by the SQUID increases with its bias current. Thus, when the SQUID is unbiased, it should not contribute to decoherence at all.

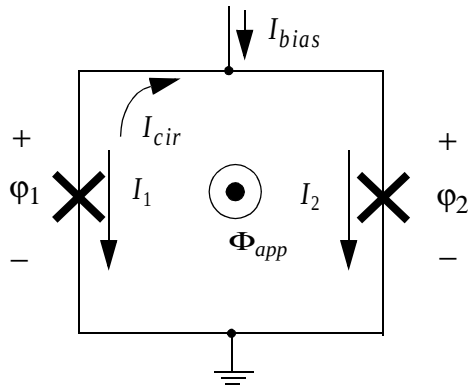

FIGURE 3. Circuit diagram of the DC SQUID.

5. Relaxation of a Coherent Quantum System During Premeasurement Entanglement

Sponsors
AFOSR grant F49620-1-1-0457 funded under the Department of Defense, Defense University Research Initiative on Nanotechnology (DURINT) and by ARDA; DOD and AFOSR; ARO GrantDAAG55-98-1-0369

Project Staff
Lin Tian, Professor Seth Lloyd, Professor Johan E. Mooij[1], Frank K. Wilhelm[1], C.H. van der Wal[1], and Professor Leonid Levitov, Professor Terry P. Orlando

Recent experiments on superconducting loops have demonstrated coherent superpositions between macroscopic quantum states. In the experiment of the superconducting persistent-current qubit, a dc SQUID measures the magnetic flux generated by the persistent currents of the macroscopic quantum states. Due to the inductive interaction between the qubit and the SQUID, the SQUID has various back effects on the qubit. For instance, the relaxation and dephasing of the qubit are limited by the noise from the environment of the dc SQUID. Here, we calculated the noise transmitted to the qubit from the environment of SQUID and analyzed its effect on qubit dynamics within the spin-boson formalism. The results can be applied to optimizing the measurement circuit for the best signal-to-noise ratio. We also studied the intrinsic limitation of the SQUID measurement scheme and developed new method to improve the measurement efficiency.

During measurement, a bias current I_b is ramped through the SQUID; and the switching current, where the SQUID switches to finite voltage state, is measured. Due to quantum fluctuation and thermal activation, the SQUID switches before the critical current and has a finite distribution. The average switching current shifts with the effective critical current and reflects the probability of the two-qubit states. In this ramping process, as the qubit and the SQUID become entangled, the noise from the environment of the SQUID affects the qubit via their inductive interaction. We calculated the noise in the Caldeira-Leggett formalism where dissipation process is described as the generalized susceptibility of an effective circuit. The method we developed can be applied to other interacting systems to study the noise problems.

The qubit dynamics is described within a master equation approach when the interaction with the environment is weak. From this approach the relaxation and decoherence of the qubit, also called the transversal relaxation and the longitudinal relaxation rates, are described by the spectrum density of the environment. As the inductive interaction induces a σ_z interaction between the qubit and SQUID environment, the qubit Hamiltonian H_0 has non-commuting σ_x component with the σ_z interaction, a transversal interaction that flips the qubit and eventually relaxes it and the qubit eigen-basis is created.

[1] Delft University of Technology, The Netherlands

This transversal interaction depends on both the tunneling between the two localized qubit states and the inductance coupling quadratically. With the renormalized spectrum density, the qubit is damped strongly by the SQUID environment. This effect prevents the measurement of the coherent oscillation between the macroscopic states with the current experimental setup.

Our study also suggests that by engineering the measurement circuit, we can optimize the spectrum density seen by the qubit and minimize the relaxation of the qubit due to various environmental fluctuations. Within the theoretical framework, various designs can be analyzed and compared.

We also studied the built-in limitation of the flux detection scheme by the dc SQUID. Our conclusion is that the direct detection of the flux of the qubit is not an efficient way of resolving the qubit states. This inefficiency is due to the fact that the flux induced in the qubit by the persistent currents is small comparing to the quantum broadening of the SQUID loop. To improve the measurement, we developed a new scheme that can resolve the qubit state in one single shot of the measurement by applying an entanglement technique before detecting the flux of the qubit.

6. Fast On-Chip Control Circuitry

Sponsors

ARO Grant DAAG55-98-1-0369 and Department of Defense University Research Initiative on Nanotechnology (DURINT) Grant F49620-01-1-0457

Project Staff

Donald S. Crankshaw, John Habif, Daniel Nakada, Professor Marc Feldman, Professor Mark Bocko, Dr. Karl Berggren

RSFQ (Rapid Single Flux Quantum) electronics can provide digital circuitry which operates at speeds ranging from 1 - 100 GHz. If these electronics can be integrated onto the same chip as the qubit, complicated control with precise timing can be applied to the qubit by on-chip elements. The following design is currently in fabrication.

An RSFQ clock can be used as the oscillator to rotate the PC qubit. This oscillator has more frequency components and less tunability than a DC SQUID, but it is easier to use in conjunction with other RSFQ components. In the following design, these components can deliver a variable frequency signal. An RSFQ clock is simply a Josephson Transmission Line ring. The transmission line propagates a pulse in its loop, which can be tapped off and used as a clock signal. Two counters and a Non-Destructive Read Out (NDRO) mem-ory cell make up the digital pulse width modulator. The signal from the clock goes to both counters and to the Read input of the NDRO. The NDRO outputs a 1 for each clock input if a 1 is stored in it, but no output for each pulse if a 0 is stored in it. The output of the counters go to the Set (which sets the NDRO to 1) and the Reset (which resets the NDRO to 0) inputs of the NDRO. The counters are equal in length (13 bits), so that after 2^{13} pulses, each one sends its output to the NDRO. By initially offsetting the counters by pre-loading them with the Offset inputs, one can set them out-of-phase with one another, thus controlling the duty cycle of the NDRO output. Since the NDRO signal has lots of har-monics, an RLC resonance filters the signal before delivering it to the qubit. The resonance filter converts the highly non-linear clock signal to a nearly sinusoidal signal.

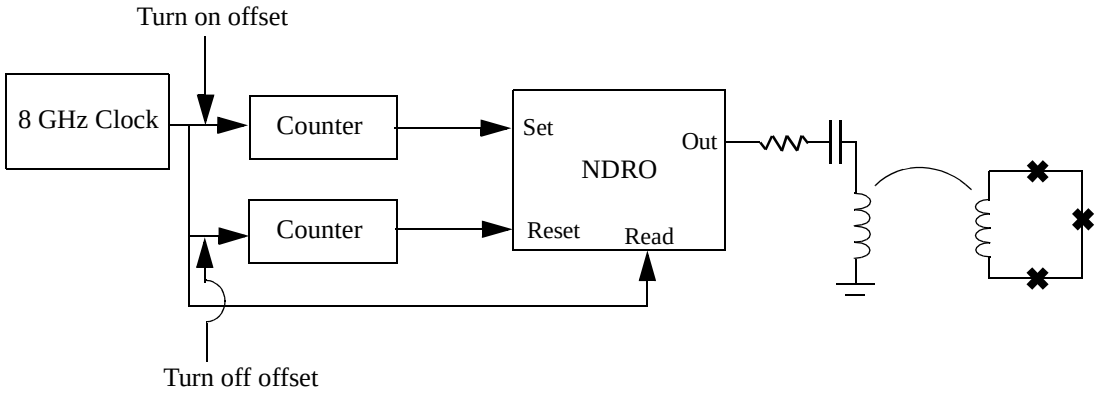

FIGURE 4. Variable duty cycle oscillator.

7. Design of Coupled Qubit

Sponsors

ARO Grant DAAD-19-01-1-0624 and Hertz Fellowship

Project Staff
Bhuwan Singh, John Habif, William Kaminsky, Professor Terry Orlando, Professor Seth Lloyd

The main requirement for the coupled qubits is that the coupled qubit system have 4 distinguishable states corresponding to 4 properly spaced energy levels.

Distinguishability here refers to the possibility of making a distinction between each of the 4 states by measurement. For a fully functioning 2-qubit quantum computer, it is necessary that the 4 qubit states that are functionally orthogonal be experimentally distinguishable. In the current design, the coupled qubits are actualized as two PC qubits weakly coupled by their mutual inductance. In the single qubit case, the DC measurement SQUID measures the state of the qubit through the flux induced by the qubit circulating current in the DC SQUID. The basic idea is unchanged for the coupled qubit system. In this case, there is one DC SQUID that measures the collective state of the coupled qubits through the total induced flux created by both qubits. For example the $|00\rangle$ state could correspond to qubits 1 and 2 both having counterclockwise circulating current. In this case, the $|11\rangle$ state would correspond to both qubits with clockwise circulating current. If the individual qubits were measurable with the DC SQUID, then the $|00\rangle$ and $|11\rangle$ states of the coupled qubit system should also be measurable because the total qubit flux induced on the DC SQUID is simply the sum of the individual qubit fluxes. The difficulty in measurement comes in differentiating the $|01\rangle$ and $|10\rangle$ states.

A difference in the measured flux from the $|01\rangle$ and $|10\rangle$ states can come from a difference in the mutual inductance between the individual qubits and the measurement SQUID and/or a difference in the magnitude of the circulating current for the two qubits. Currently, it is not practical to achieve the separation of flux states from adjusting mutual inductance values. Therefore, the approach has been to create two qubits with differing circulating current magnitudes. The magnitude of the circulating current is determined by the size of the junctions. Our analysis shows that there are 6 acceptable qubit parameter choices given the fabrication constraints for a single qubit. Since there are 2 qubits in the coupled qubit system, there are a total of 15 possible “distinct” coupled qubit combinations. Not all of these 15 possibilities are practical, because some still require rather large qubit-SQUID coupling for distinguishability between the $|01\rangle$ and $|10\rangle$ states. The qubit-qubit and qubit-SQUID mutual

inductance are parameters that can be varied through choices in geometry. As in the single qubit case, there are inherent tradeoffs in deciding on the appropriate size of the coupling.

The need for properly spaced energy levels comes from the mode of operation of the qubit. The qubits will be rotated, be it individually or collectively, through RF radiation of the appropriate frequency. In the first round of experiments, the signal will come from an off-chip oscillator. For the full functionality of the couple qubit system, it is required that there be 4 non-degenerate energy levels corresponding to the $|00\rangle$, $|01\rangle$, $|10\rangle$, and $|11\rangle$ states and that the 6 possible state transitions have sufficiently different resonant frequencies. If these conditions are met, then pulses with the appropriate linewidth would be able to do universal quantum computation on the 2-qubit system, including the "CNOT" operation. Following along the previous assumption that the coupled qubit system is accurately described as two individual qubits with weak mutual inductive coupling, it should be clear that the $|00\rangle$ and $|11\rangle$ states (corresponding to both qubits in the ground or excited states) should be well separated in energy. To meet the other requirements on the energy levels, the qubit-qubit mutual inductive energy needs to be sufficiently large and the qubits need to have different junction sizes. The latter requirement is already necessitated by the measurement limitations. The former represents another tradeoff in the design, as there are problems if the coupling is too strong. Beyond the aforementioned desiderata, it is necessary that the magnitude of these resonant frequencies be practical for experiments.

For the current fabrication run, there are 6 coupled qubit designs. An effort was made to span the acceptable parameter space for the tradeoffs mentioned above.

8. Engineering Josephson Oscillators

Sponsors
National Science Foundation Grant DMR 9988832
NSA and ARDA under ARO Grant DAAG55-98-1-0369

Project Staff
Donald S. Crankshaw, Enrique Trías, Professor Terry P. Orlando

As the telecommunications revolution pushes for denser utilization of the spectrum, there is a need to develop inexpensive sources and detectors that operate in the 100 GHz to several THz range. It is precisely in this range that Josephson junctions provide an almost ideal solid state, current controllable source.

Arrays of junctions provide for relatively large power but due to non-linearities they can exhibit diverse complex spatiotemporal patterns. Experiments, simulations, and analysis were performed on a broad range of discrete arrays of Josephson-junction oscillators in order to understand their ability to produce coherent radiation. Networks ranging from single square and triangular plaquettes to one- and two-dimensional arrays were studied. In each array, the junctions are identical, and the arrays are driven by dc bias currents. Although few analytical results are known for these systems, we study the technically interesting solutions which can be represented as traveling waves. It is in this mode that the devices can be used as submillimeter wave sources.

Using the mathematical technique of harmonic balance it is possible to create an equivalent linear circuit of a Josephson network that is operating in a traveling wave mode. Though the non-linearity of the system allows for mixing of all the harmonics, in underdamped systems we find that the first harmonic is orders of magnitude stronger than the rest. In general, any variable can be decomposed in terms of its dc and ac spectrum. If we further restrict the ac component to a single frequency as suggested by our simulations, then the branch current and voltage across a junction can be written as:

$$
\begin{aligned}
I &= I_{DC} + i_{ac} e^{j\omega t} \\
V &= V_{DC} + v_{ac} e^{j\omega t} \\
I_c &= e^{jk}, \\
I_M &= \frac{v_{ac}}{j\omega} \frac{e^{-jk}}{2}.
\end{aligned}
\tag{3}
$$

Our equivalent circuit then consists of a dc bias circuit and a mixing circuit that creates the first harmonic. Figure 5 depicts the equivalent circuit. Here k represents the phase difference between the first harmonic and the rotating part of the Josephson oscillation, and the mixing current, I_M, represents the nonlinear interaction between them. This equivalent circuit makes it possible to use powerful circuit theoretic tools to understand a Josephson network.

This model has been used to design a matched load detector. A Josephson junction can be used to detect and measure power, and designing a detector to match the impedance of an array allows us to measure the power produced by the array. As shown in Figure 6, experiments measuring the power which an array of 54 overdamped junctions delivers to an impedance match load attest to the usefulness of our model, giving a strong qualitative correlation between the predicted and measured power for varying magnetic flux (measured in units of frustration, the number of flux quantum per unit cell).

Currently, much of our oscillator work is designed to drive quantum circuits, such as the qubit and the quantum ratchet. The oscillators designed for this work are less focused on maximum power than minimum decoherence, meaning that designs may benefit from deliberately unmatched impedances. The exacting requirements of this application further test the accuracy of our model in a challenging regime.

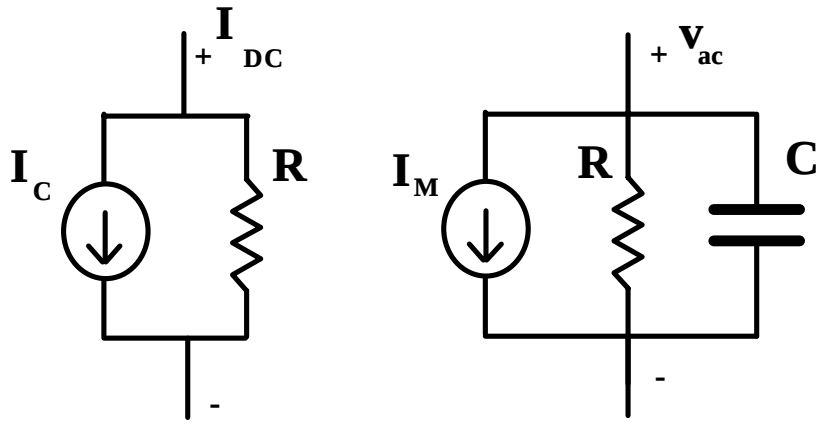

FIGURE 5. Equivalent circuit for a Josephson junction in a voltage state and with a single harmonic. Non-linearity is captured by I_M which is a mixing current that describes the interaction between the rotating Josephson phase and its first harmonic.

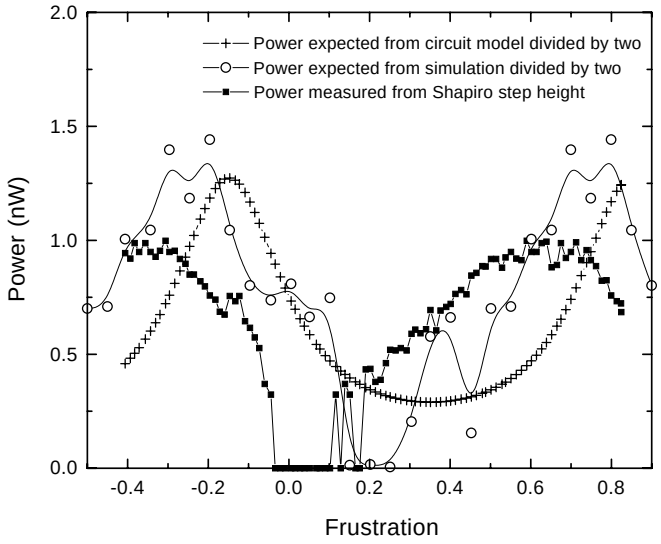

FIGURE 6. The power produced by the array, experimental measurements compared to nonlinear simulation and linear circuit model predictions. The array is biased at V_{arr} = 0.1035 mV.

9. Type II Quantum Computing Using Superconducting Qubits

Sponsor
AFOSR grant F49620-1-1-0457 funded under the Department of Defense, Defense University Research Initiative on Nanotechnology (DURINT)

Project Staff
Professor Terry Orlando, David Berns, Dr. Karl Berggren (Lincoln Laboratory), Jay Sage (Lincoln Laboratory), Jeff Yepez (Air Force Laboratories)

Most algorithms designed for quantum computers will not best their classical counterparts until they are implemented with thousands of qubits. By all measures this technology is far in the future. On the other hand, the factorized quantum lattice-gas algorithm (FQLGA) can be implemented on a type II quantum computer, where its speedups are realizable with qubits numbering only in the teens. The FQLGA uses a type II architecture, where an array of nodes with only a small number of coherently coupled qubits is connected classically (incoherently). It is the small number of coupled qubits that will allow this algorithm to be of the first useful quantum algorithms ever implemented.

The algorithm is the quantum mechanical version of the classical lattice gas algorithm, which can simulate the Navier-Stokes equation with unconditional stability. This algorithm was developed in the 1980's and has been a powerful fluid dynamic simulation model ever since. It is a bottom-up model where the microdynamics are governed by only three sets of rules, unrelated to the microscopic physics of the system. The quantum algorithm has all the properties of the classical algorithm but with an exponential speedup in running time.

We are currently looking into the feasibility of implementing this algorithm with our superconducting qubits, with long-term plans of constructing a simple type II quantum computer. Current questions being addressed are the following:

> With what accuracy can our qubits be set into a specific quantum state while coupled to other qubits and measurement devices? This will be the limiting factor in the accuracy of our fluid simulations. Since ensemble measurements are performed in the algorithm, should these repeated measurements be performed repeatedly in time or in space? Can we design our system so that the qubits' Hamiltonian will force them to evolve the same as they would under the specified unitary transformation for the algorithm? This is what gives the quantum algorithm its advantage in running time.

10. Vortex Ratchets

Sponsorship
National Science Foundation Grant DMR 9988832
Fulbright/MEC Fellowship

Personnel
Dr. Kenneth Segall, Dr. J.J. Mazo, Professor Terry P. Orlando

The concept of a *ratchet* and the *ratchet effect* has received attention in recent years in a wide variety of fields. Simply put a ratchet is formed by a particle in a potential which is asymmetric, i.e. it lacks reflection symmetry. An example is the potential shown in Fig.1, where the force to move a particle trapped in the potential is larger in one direction (the left) and smaller in the other. The ratchet effect is when net transport of the particle occurs in the absence of any gradients. This can happen when the system is driven out of equilibrium, such as by an unbiased AC force or non-gaussian noise. Ratchets are of fundamental importance in biological fields, for study of dissipation and stochastic resonance, in mesoscopic systems, and in our case in superconducting Josephson systems. The key questions are to study how the transport of the particle is affected by the ratchet potential

In our group we study the ratchet effect in circular arrays of superconducting Josephson Junctions. In such arrays magnetic vortices or kinks can be trapped inside and feel a force when the array is driven by an external current. The potential that the vortex feels is given by a combination of the junction sizes and the cell areas; by varying these in an asymmetric fashion we can construct a ratchet potential for a vortex. The picture in Fig. 1 is of one of our fabricated circular arrays; the potential shown in Fig. 1 is the numerically calculated potential for a kink inside the array. We have verified the ratchet nature of the potential with DC transport measurements, published in early 2000.

This work is now moving in two new directions: smaller junction arrays where quantum effects are important and AC biasing or so-called rocking ratchets. A quantum ratchet will display new behavior as the temperature is lowered, as both the ratchet potential and quantum tunneling can contribute to the kink transport. We have designed and fabricated such arrays and are presently testing them. AC biasing of our arrays will cause the vortex to move and such vortex motion results in a net DC voltage across the array. In Fig. 2 we demonstrated this so-called rocking ratchet, with numerical simulations and in the adiabatic limit of our previous results (DC measurements). The particle current as a function of AC biasing provides key information on the form of the ratchet potential. We plan to move in the direction of higher frequency, where more interesting structure can develop. All of these experiments are important to verify the different aspects of the ratchet effect.

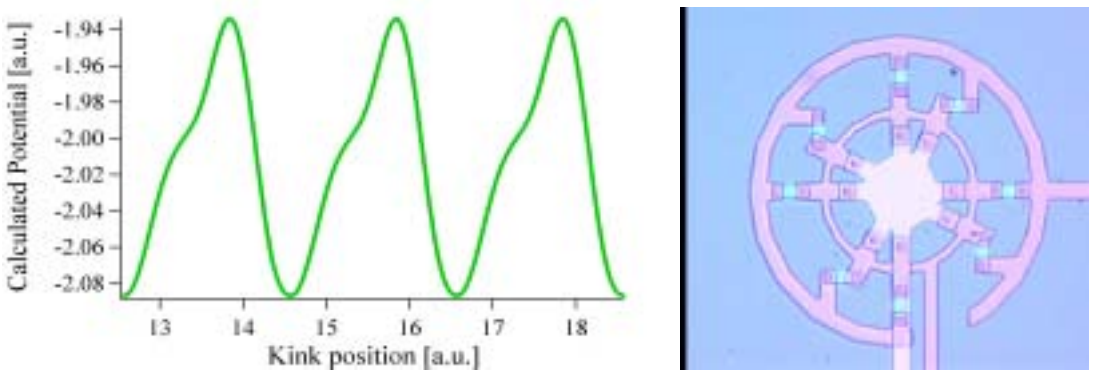

Fig.1: A ratchet potential and its realization in a Josephson array. The array has alternating junction sizes and plaquete areas to form the asymmetric potential for a vortex trapped inside the ring. The outer ring applies the current such that the vortex transport can be measured. The potential is numerically calculated for the array parameters.

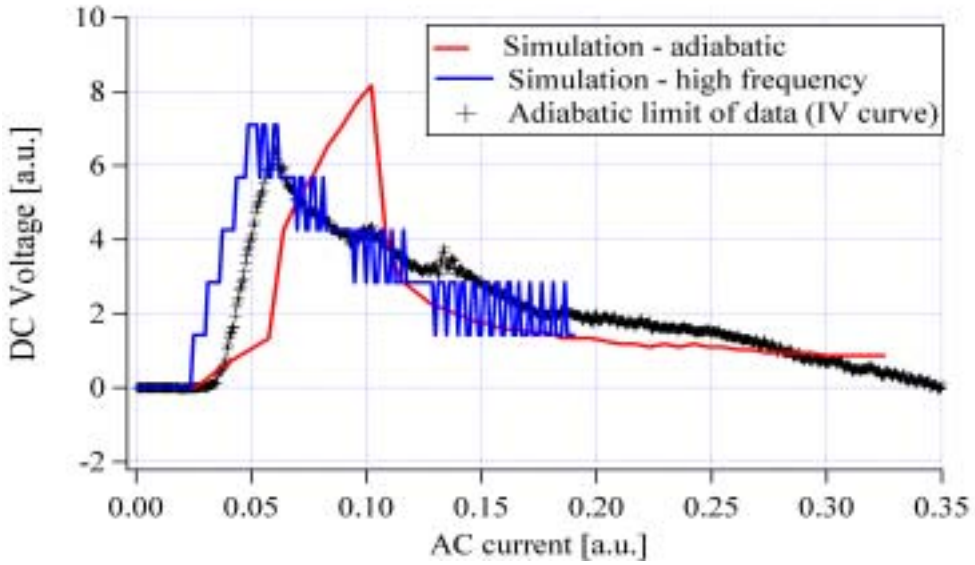

Fig. 2: Simulation and experiment for the so-called rocking ratchet, where the ratchet is subjected to an unbiased AC force. The vertical axis is the DC voltage across the circular array and is proportional to the particle (vortex) velocity. The horizontal axis is the amplitude of the AC applied force (current).

11. Interaction between discrete breathers and other non-linear modes in Josephson arrays

Sponsorship
National Science Foundation Grant DMR 9988832
Fulbright/MEC Fellowship

Personnel
Dr. Kenneth Segall, Dr. J.J. Mazo, Professor Terry P. Orlando

Linear models of crystals have played a fundamental role in developing a physical understanding of the solid state. However, many phenomena are unexplained untill one considers non-linear interactions. One particularly interesting phenomena is that of *discrete breathers*, which are time periodic, spatially localized modes. In a crystal a discrete breather is localized in that a few atoms are vibrating while the neighboring atoms stay still. Josephson junctions are a solid state realization of non-linear oscillators and they can experimentally be coupled in various ways using standard lithographic fabrication techniques. In figures 1A and 1B we show a regular array of Josephson junctions, denoted by x's, which are driven by a uniform current (driving current not shown). Each junction is governed by equations isomorphic to a damped pedulum; the phase of the pendula is equivalent to the superconducting phase difference across the junction. A discrete breather is shown in 1B, where a few of the junctions have their phases rotating in time while the others do not. Experimentally a rotating phase corresponds to a net DC voltage, which can be easily measured. Breathers in Josephson arrays have been studied in previous work in our group here at MIT.

In Fig. 1A we demonstrate another kind of non-linear mode, a *moving vortex*. This is mathematically equivalent to a kink or solitonic mode. Vortices in Josephson arrays carry a quantum of magnetic flux and have been studied extensively in superconducting systems. A vortex corresponds to a 2□ phase shift in the phases of the vertical juntions in the ladder; when a uniform current is applied the vortex moves down the ladder. As the vortex passes a given junction it causes its phase to undergo a rotation and thus create a voltage. This is indicated by the time sequence shown in Fig. 1A.

Our work is aimed at studying the interaction of discrete breathers with other kinds of non-linear modes, like a moving vortex. Such questions are of fundamental importance for the Non-linear Dynamics community. In Fig. 2 we show a mathematical simulation of a collision between a vortex and a breather. The vertical axis is the junction number in the array; the array in the simulation has 60 junctions. The horizontal axis is time. The color indicates the junction voltage or rotation speed, with blue indicating low voltage and red indicating high voltage. Initially there is a breather located about junction 10 and a vortex located in junction 45. As time proceeds the vortex moves toward the breather and eventually collides with it. The result of the collision is that the breather acts as a pinning center for the vortex. As time proceeds further (not shown) the vortex will eventually depin and cause the breather to decay into a different mode. We have also seen other collision scenarios in our simulations, such as ones where the breather is destroyed or where the breather pins a train of moving vortices. We are also looking for such behavior experimentally, with fabricated junction arrays and DC electronics.

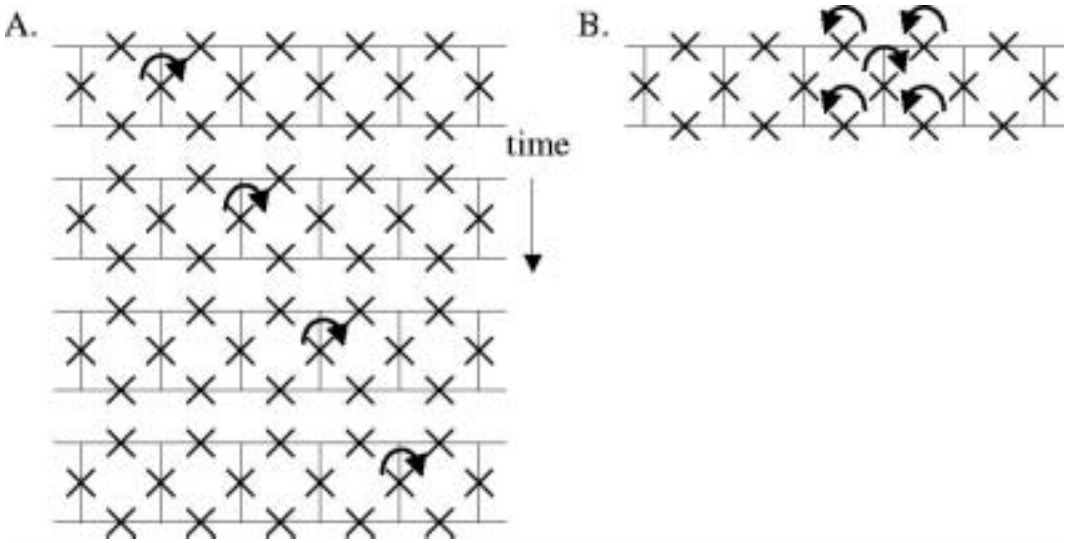

Fig. 1: Representation of two different non-linear modes in a Josephson Ladder: (a) Moving vortex: The vortex causes the phase of a junction to rotate as it passes by. (b) Discrete breather: A few junctions have their phases continually rotating while the neighboring ones do not.

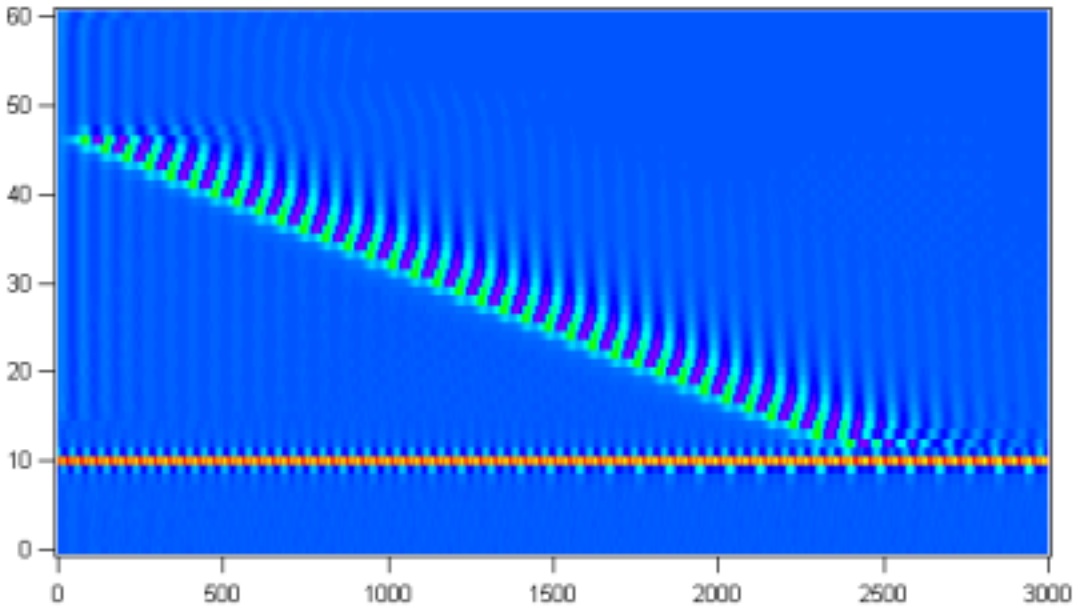

Fig. 2: Interaction of a breather with a moving vortex. Time (in arbitrary units) is on the horizonal axis, the junction number is on the vertical axis, and the color indicates the junction voltage (red=high, blue=low). The vortex starts in junction 45 and moves toward the breather, which is in junction 10. The vortex collides with the breather and is pinned by it, with the breather surviving at later times.

Journal Articles, Published

T. P. Orlando, S. Lloyd, L. S. Levitov, K. K. Berggren, M. J. Feldman, M. F. Bocko, J. E. Mooij, C. J. P. Harmans, C. H. van der Wal, "Flux-based Superconducting Qubits for Quantum Computation," presented at the 5th European Conference on Applied Superconductivity, Copenhagen, August 2001.

T. P. Orlando, Lin Tian, D. S. Crankshaw, S. Lloyd, C. H. van der Wal, J. E. Mooij, F. Wilhelm, "Engineering the Quantum Measurement Process for the Persistent Current Qubit," presented at SQUID 2001, Sweden, August 2001.

D. S. Crankshaw, T. P. Orlando, "Coherent Driving of the Persistent Current Qubit,"

D. S. Crankshaw and T. P. Orlando, "Inductance effects in the persistent current qubit," *IEEE Trans. on Applied Superconductivity:* Volume: 11 Issue: 1 Part: 1 p: 1006 -1009, March 2001

D.S. Crankshaw, E. Trias, T.P. Orlando, "Magnetic flux controlled Josephson array oscillators," *IEEE Transactions on Applied Superconductivity,* Volume: 11 Issue: 1 Part: 1 p: 1223 -1226, March 2001

K. Berggren, D. Nakada, T.P. Orlando, E. Macedo, R. Slattery, and T. Weir, "An integrated superconductive device technology for qubit control," submitted for publication.

L. Tian, S. Lloyd, T.P. Orlando, "Decoherence and relaxation of a superconducting quantum bit during measurement," May 31, 2001

T.P. Orlando, L. Tian, S. Lloyd et al, “Engineering of Measurement Induced Noise”, to appear in *Physica C*, (2001);

L. Tian, S. Lloyd and T.P. Orlando, “Decoherence and Relaxation of Superconducting Persistent-Current Qubit During Measurement “, accepted by *Phys. Rev. B.* (2002);

L. Tian, S. Lloyd and T.P. Orlando, “Environmental Noise on a Qubit Through Entanglement with a Quantum Circuit”, submitted to ICQI, June 2001.

L. Tian and S. Lloyd, “Resonant cancellation of off-resonant effects in a multilevel qubit”, *Phys. Rev. A* 62, RC050301 (2000);